Arch. Pharm. Res. (2016) 39:912–925
DOI 10.1007/s12272-016-0744-6

Archives of Pharmacal Research
www.springer.com/12272

RESEARCH ARTICLE

HPLC–DAD–MS/MS profiling of standardized rosemary extract and enhancement of its anti-wrinkle activity by encapsulation in elastic nanovesicles

Shahira M. Ezzat[1] · Maha M. Salama[1] · Aliaa N. ElMeshad[2] · Mahmoud H. Teaima[2] · Laila A. Rashad[3]

Received: 29 October 2015 / Accepted: 17 April 2016 / Published online: 23 April 2016

Abstract The anti-wrinkle activity of defatted rosemary extract (DER) was assessed, and its effect was optimized by encapsulation in transferosomes (TFs). DER was standardized to a rosmarinic acid content of 4.58 ± 0.023 mg% using reversed-phase high performance liquid chromatography (Rp-HPLC), and its components were identified by HPLC-diode array detection-tandem mass spectrometry. In vitro free radical scavenging assays showed DER had high free radical scavenging activity against 2,2-diphenyl-2-picryl hydrazyl, 2,2′-azino-bis(3-ethylbenzothiazoline-6-sulfonic acid), and superoxide radicals. DER also inhibited bleaching of β-carotene with high Fe(III) and Fe(II) chelating ability. In vivo anti-wrinkle activities of topically applied DER (20, 50, and 100 mg) and a TF formulation (TF4, 20 mg of DER) were evaluated in UVB-irradiated mice using a wrinkle scoring method, metalloproteinase (MMP) expression, and histopathology. Among the nanovesicles, TF4 was the most deformable, and had an acceptable size and encapsulation efficiency and enhanced permeation of DER through rat skin compared with unencapsulated DER. DER (50 and 100 mg) and TF4 significantly inhibited MMP-2 and MMP-9 expression and improved wrinkle scores. DER and TF4 moderately decreased epidermal thickness without pigmentation. DER is a potent natural antioxidant for combating skin aging. Moreover, encapsulation of DER in TFs will enhance its skin permeation and anti-wrinkle activity.

Keywords Rosemary · HPLC–DAD-MS/MS · Transferosome · Antioxidant · Anti-wrinkle · Skin permeability

✉ Shahira M. Ezzat
shahira.ezzat@pharma.cu.edu.eg

[1] Department of Pharmacognosy, Faculty of Pharmacy, Cairo University, Kasr El-Ainy St., Cairo 11562, Egypt

[2] Department of Pharmaceutics and Industrial Pharmacy, Faculty of Pharmacy, Cairo University, Cairo, Egypt

[3] Department of Medical Biochemistry, Faculty of Medicine, Cairo University, Cairo, Egypt

Introduction

There are many factors, both genetic and environmental, that lead to aging of the skin. Environmental exposure to ultraviolet (UV) radiation results in skin roughness, fine lines, sagging, irregular pigmentation, and decreased skin elasticity. Cumulative exposure to UV irradiation is one of the leading causes of these skin changes. UV irradiation damages skin cells through photochemical generation of reactive oxygen species (ROS) that damage nucleic acids, lipids, and proteins, including collagen. Many of these alterations in the extracellular matrix are mediated by the matrix metalloproteinases (MMPs). MMPs are involved in extracellular matrix remodeling and play important roles in morphogenesis, angiogenesis, arthritis, skin ulceration, tumor invasion, and photo-aging (Birkedal-Hansen 1995; Fisher et al. 1996). Skin damage caused by chronic UVB irradiation is always associated with increases in skin thickness and wrinkling in addition to reduction of skin elasticity, and these effects are caused by an increase in expression of the MMPs; MMP-2 and MMP-9 (Bissett et al. 1987). MMP-2 and MMP-9 degrade collagen and are suggested to be UV-induced aging factors (Fisher et al. 1996).

Various antioxidant compounds have been tested to determine their ability to protect the skin from photo-aging (Pinnell 2003). For effective photo-protection of the skin, a

certain amount of antioxidant should be applied to the skin. However, the effectiveness of active constituents is limited by the delivery of drugs in topical preparations because of the barrier properties of the skin, which hinder drug permeation. In addition, topical preparations have relatively poor stability on direct exposure to UV light. Hence, selection of an appropriate carrier is extremely important to increase drug permeation (Verma et al. 2003), flux (Jia-You et al. 2004), and to protect the drug from photodegradation. Recently, Alzomor et al. (2015) studied the anti-wrinkle activity of rosemary extract formulated in cream and gel forms.

Liposomes (LPs) are promising carriers for enhancing skin permeation because they have high membrane fluidity (Mura et al. 2007). LPs can deliver various types of hydrophilic and lipophilic drugs, proteins, and macromolecules through the skin (Manconi et al. 2011). Transferosomes (TFs) are elastic liposomes prepared from phospholipids and edge activators (Zhang et al. 2012). Single-chain surfactants with high radius of curvature are often used as edge activators since they destabilize the lipid bilayers of the vesicles and increase the deformability of the bilayers. These ultra-deformable carriers have the ability to cross intact skin aided by the naturally occurring transcutaneous hydration gradient. The hydrotaxis of vesicles permits the carrier to move more than 50 % of a drug epicutaneously administered across the skin barrier (Cevc et al. 1998).

Rosmarinus officinalis L. (rosemary) is a well-known herb with many medicinal uses and is regarded as having memory-enhancing abilities (Calabrese et al. 2000). It is one of the most common herbs used in skin care products because it is rich in active antioxidant compounds (Inatani et al. 1983; Frankel et al. 1996) as well as microelements and nutrients, which improve skin quality (Koleva et al. 2002; Cao et al. 2005; Muñoz-Muñoz et al. 2013).

In the present study, a standardized defatted rosemary extract (DER) was prepared and then profiled by high performance liquid chromatography (HPLC)-diode array detection (DAD)-tandem mass spectrometry (MS/MS). The antioxidant capacity of the standardized extract was investigated in different in vitro assays. The aim of this research was to enhance the permeation of DER across the skin by formulation in non-invasive ultra-deformable nanovesicles prepared using natural phospholipids and edge activators. Finally, the in vivo anti-wrinkle activities of the standardized DER alone and that of the nanovesicle formulation were compared by measuring the inhibition potential of MMP-2 and MMP-9 expression in mice, and using the results to calculate a wrinkle score. The results were supported by histopathological studies.

Materials and methods

Plant material and preparation of DER

Aerial parts of *R. officinalis* L. were obtained from the Experimental Station of Medicinal, Aromatic and Poisonous Plants, Pharmacognosy Department, Faculty of Pharmacy, Cairo University, Giza, Egypt (voucher specimen 2014067). The aerial parts were air dried and ground to a powder, and samples of the powder (2 kg) were defatted using *n*-hexane in a Soxhlet extractor, and then extracted by percolation with 70 % ethanol (3 × 5 L). The ethanol was evaporated under reduced pressure to yield 350 g of DER.

Materials

β-carotene, linoleic acid, 2,2-diphenyl-2-picryl hydrazyl (DPPH), gallic acid, nitro blue tetrazolium, 2,2′-azino-bis(3-ethylbenzothiazoline-6-sulfonic acid) (ABTS) diammonium salt, rosmarinic acid, carnosic acid, L-α-phosphatidylcholine [egg yolk] (PC), cholesterol (Chol), sodium deoxycholate (SDC), sorbitan monostearate (Span 60), and Triton X-100 were obtained from Sigma-Aldrich (St. Louis, Missouri, United States). Polyoxyl 35-castor oil (Cremophor EL) was purchased from Sasol Olefins & Surfactants GmbH (Hamburg, Germany). Solvents for HPLC analysis were obtained from Sigma-Aldrich (St. Louis, Missouri, United States).

Methods

HPLC standardization of the DER

Sample preparation

An ethanol (70 %, 3 × 5 mL) extract of the rosemary was prepared by sonication of 2 g of the powdered aerial parts in a stoppered conical flask. The extract was filtered into a volumetric flask (25-mL capacity) and the volume was adjusted to the mark with 70 % ethanol.

Reversed-phase HPLC analysis

The method of Troncoso et al. (2005) was used for HPLC with a LaChrom system (Hitachi High Technologies, Tokyo, Japan), an XTera RP18 column (46 × 250 mm, 5-µm particle size, Waters, Milford, MA), a UV–visible (UV–Vis) detector (L-7420, Hitachi), and a data station with D-7000 software (Hitachi High Technologies). The temperature and pressure were 30 °C and 2895.48 kPa,

respectively. The sample was eluted using an isocratic elution with a mobile phase of 30 % acetonitrile, 70 % acetonitrile aqueous solution (2.5 % volume fraction), and formic acid (0.5 % volume fraction) at a flow rate of 1 mL/min. The sample injection volume was 20 µL. The detection wavelength for the UV–Vis detector was 230 nm. The retention time of the rosmarinic acid was 5.572 min (Fig. 1B).

Evaluation of precision and standard curve construction

A stock solution was prepared by dissolving rosmarinic acid in methanol (0.1 µg/mL). Aliquots (1, 2, 4, 6, 8, 10, 12, 14, 16 and 18 ng/mL) of this solution were diluted with methanol, sonicated for 30 min, and filtered through 0.45-µm membrane filters (Millipore, Thermo Fisher Scientific, Waltham, MA). The intraday precision of the analytical method was

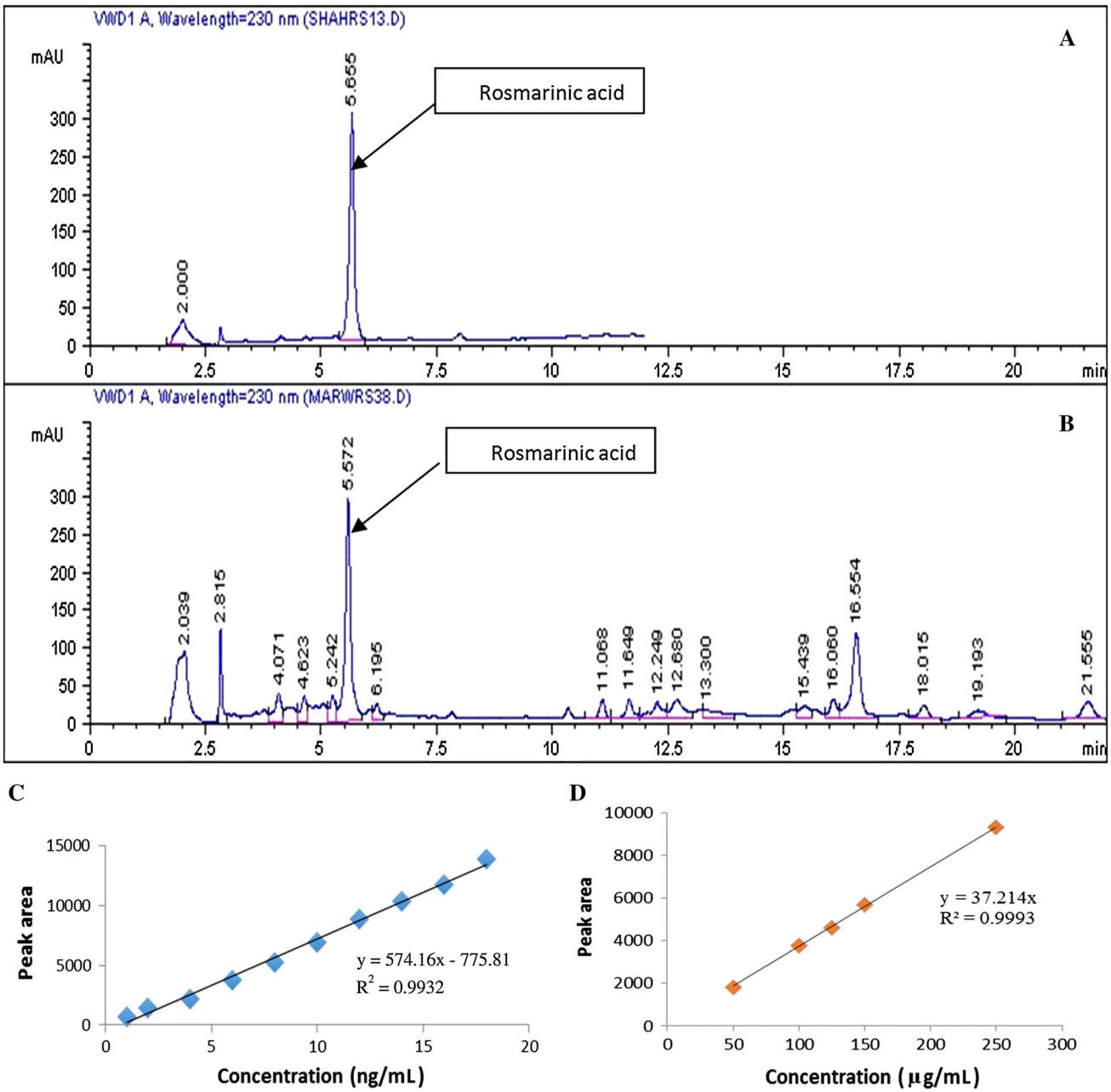

Fig. 1 HPLC analysis of DER: **A** HPLC chromatogram of the standard rosmarinic acid (RA) (Rt 5.57 min), **B** HPLC fingerprint for DER (1.25 mg/ml), **C** standard calibration curve of rosmarinic acid (concentration in ng/ml) and **D** standard calibration curve of rosmarinic acid (concentration in µg/ml)

evaluated by analyzing samples of DER with different concentrations (4, 16, and 18 µg/mL) in triplicate on the same day. The interday precision was evaluated using the same solutions on three consecutive days (Fig. 1C).

Another stock solution (25 µg/mL) was prepared by accurately weighing 6.25 mg of rosmarinic acid into a 25-mL volumetric flask and dissolving in methanol. Aliquots of this solution were diluted to 100, 125, 150, 200, and 250 µg/mL. A standard curve was constructed using these solutions. Each sample was analyzed in triplicate. This curve was used for standardization of DER (Fig. 1D).

HPLC–DAD-MS/MS profiling of DER

The analysis was carried out using the method of Mulinacci et al. (2011) on a HP 1100L system, with a UV detector coupled to a mass spectrometer (HP 1100 MSD) with an API/electrospray interface (Agilent Technologies, Santa Clara, CA). The column was a Fusion RP18 (150 × 3.9 mm, 4-µm particle size, Phenomenex, Torrance, CA). UV–Vis spectra were recorded in the range 200–500 nm, and chromatograms were acquired at 284 and 330 nm. The mass spectra were recorded in negative and positive electron ionization modes with fragmentation energy between 80 and 180 V.

In vitro antioxidant assays of the standardized DER

DPPH radical scavenging was conducted according to a modification (Delazar et al. 2004) of the method of Takao et al. (1994). The $ABTS^{\cdot+}$ scavenging ability was measured spectrophotometrically at $\lambda = 734$ nm (Ozgen et al. 2006). Scavenging of superoxide radicals was evaluated using the alkaline dimethyl sulfoxide method (Elizabeth and Rao 1990). The radical scavenging effect of DER in each case was calculated using the following equation:

$$\% \text{ Inhibition } = [(A_B - A_A)/A_B] \times 100$$

where A_B is the absorbance of the control sample, and A_A is the absorbance of the test sample after 30 min. The IC_{50} value was calculated as the concentration (µg/mL) of test sample that resulted in quenching of 50 % of the UV absorption of each tested radical.

The anti-lipid peroxidation activity of DER was determined by the linoleic acid/β-carotene bleaching assay (Kumaran and Kumaran 2006). The percentage of bleaching inhibition ($I_{\text{bleaching}}$ %) was calculated using the following equation:

$$I_{\text{bleaching}}(\%) = (\text{Absorbance after 2 h of assay} / \text{Initial absorbance}) \times 100$$

In addition, ferric reducing ability of DER was evaluated (Tsai et al. 2011). Experiments were performed in triplicate and the average absorption for each concentration was recorded. Gallic acid was used as a positive control.

Preparation of transferosomes and conventional LPs

TFs and LPs were prepared by the solvent evaporation method (Bangham and Horn 1964). DER (20 mg) was loaded into the TFs and LPs to prepare different formulations. For the TFs, DER, PC and the surfactant were dissolved in 3 mL of a chloroform:methanol mixture (1:1, *v/v*). The solvent was evaporated under reduced pressure at 60 °C and 60 rpm. The lipid film was hydrated with phosphate buffered saline (PBS, pH 7.4) in a bath sonicator (S30H Elmasonic, Elma Schmidbauer GmbH, Singen, Germany) at 50 °C for 5 min. For the LPs, DER, PC and Chol were dissolved in the solvent mixture as above and the same procedure was followed (Table 2).

Characterization of vesicles

Encapsulation efficiency TFs or LPs were separated from free DER by ultracentrifugation at 4 °C and 25,356.24 × *g* for 1 h (Heraeus Megafuge 1.0R, Thermo Fisher Scientific). The vesicles were disrupted using Triton X-100 (0.5 % mass fraction), and the concentration of liberated DER was estimated by HPLC using the above method.

Vesicular size and charge The sizes and charges of the TF and LP vesicles were measured by a Zetasizer ZS (Malvern Instruments, UK) at 25 °C. The polydispersity index, which is a measure of the size distribution, was determined.

Deformability index Elasticity was determined by the extrusion method (Modi and Bharadia 2012). The vesicles were extruded through a polycarbonate filter (50 nm, Thermo Fisher Scientific) at 250 kPa (Haug Kompressoren AG, St. Gallen, Switzerland), and the time taken for extrusion was recorded. The elasticity of the vesicle membrane, expressed as the deformability index (DI), was calculated using an established method (Gupta et al. 2005).

The best performing TF in terms of the above characterization tests was further investigated for its morphology, in vitro skin permeation and in vivo anti-wrinkle activity.

Morphology

The shapes of the TFs and LP were studied using a light microscope (Leica Microsystems, Wezlar, Germany), transmission electron microscope (1230, JEOL, Tokyo, Japan) at 80 kV. Atomic force microscopy was performed using a P9 XPM Systems Digital Control Platform and

Nova software (AFM, Solver Next, NT-MDT Co, Moscow, Russia). The measurements were performed in non-contact mode with a NSG10/TiN series cantilever which was a part of the AFM (AFM, Solver Next,NT-MDT Co, Moscow, Russia) (1.6 × 3.4 mm) with a resonant frequency of 193 kHz and force constant between 3.08 and 37.6 N/m.

Skin permeation study

This experiment was carried out using a Franz diffusion cell (cross-sectional area 4.19 cm^2) mounted with skin from newborn rats to avoid hair shaving. The rats were flayed in the animal house of Faculty of Pharmacy, Cairo University. The steps of skin removal was approved by the Ethics Committee of Faculty of Pharmacy, Cairo University. The receptor medium was 25 mL of PBS (pH 7.4) containing 2 % sodium lauryl sulfate (w/w) to provide sink condition i.e. to increase the solubility of DER in PBS and ensure DER permeation through the rat skin. Measurements were performed at 37 °C and 400 rpm using 0.1 mL of a TF or LP suspension, which was placed in the donor cell at ambient temperature. The cumulative amount of extract that permeated through the skin after 24 h (Q_{24}) was calculated using HPLC analysis. The rate of permeation (R) was calculated from the slope of the linear portion of the plot, while the lag time (L_t) was determined by extrapolation of the linear portion of the plot to the abscissa. The permeation experiment was repeated using 0.1 mL of PBS containing an amount of DER equivalent to that in the TF and LP, and the results were used to compare the effect of nanovesicle formulations on permeation of DER through rat skin.

Skin retention study

For sample preparation, skin was homogenized using Heidolph DIAX 900 homogenizer (Sigma-Aldrich, St. Louis, Missouri, United States) with 10 mL of acetonitrile, and filtered through a 0.22-μm membrane filter. The amount of DER retained in the skin was determined by HPLC using the method detailed above and rosmarinic acid as the marker.

In vivo anti-wrinkle activity

Animals

Thirty-five male Swiss albino mice weighing 25 ± 5 g were obtained from the animal house of the National Research Center (Giza, Egypt). All experimental procedures were conducted in accordance with internationally accepted principles for laboratory animal use and care and were approved by the Ethics Committee, Faculty of Pharmacy, Cairo University, Cairo, Egypt (PI 1421). The experiment was carried out in accordance with recommendations for the proper use of animals (National Institutes of Health guide for the care and use of laboratory animals, NIH Publications No. 8023, revised 1978). All experiments were performed during the light phase of a light/dark cycle that was started 1 week after acclimatization. Mice had free access to food and water before the experiments.

The mice were divided into seven groups. Group I was the control group. Group II mice were irradiated with a UVB lamp but were not treated with DER in any form, and served as a positive control. Groups III, IV and V mice were UVB-irradiated and treated topically with 20, 50 or 100 mg of DER, respectively. Groups VI and VII mice were UVB-irradiated and treated topically with TF4, which contained 20 mg of DER, or non-medicated TF4 without DER respectively.

To induce wrinkle formation in the skin of the mice, their backs were shaved and they were placed under a UVB lamp (15 W, λ 254 nm, UV intensity 100 mW/cm^2; Ieda Boeki Co., Tokyo, Japan) for 5 min daily for 15 weeks. The period of irradiation was varied to control the UVB energy applied to the dorsal region. The minimal erythema dose for each mouse was about 36 mJ/cm^2. Wrinkles were observed macroscopically in the dorsal region from about 7 weeks after the initiation of UVB irradiation (Sumiyoshi and Kimura 2009). Simultaneously, DER (20, 50 or 100 mg) or TF4 (non-medicated or containing 20 mg of DER) were applied topically twice daily for 15 weeks on the shaved skin of mice in the relevant groups.

Measurement of skin wrinkles in UVB-irradiated mice

To evaluate skin wrinkles, each mouse was anesthetized with an intraperitoneal injection of pentobarbital (50 mg/kg). At the end of the 15th week, the UVB-irradiated dorsal area (site of wrinkles) of each mouse was examined and scored using Bissett's grading scale (1987). Higher scores indicated more wrinkle formation and deeper wrinkles. After the animals were sacrificed, determination of MMP gene expression in mouse skin was performed using the real-time quantitative polymerase chain reaction (qPCR). This involved RNA isolation, reverse transcription, qPCR assay development, qPCR experiment, and data analysis (Sumiyoshi and Kimura 2009).

Histological examination in UVB-irradiated mice

Dorsal skin samples (about 3 cm^2) were fixed in 10 % buffered formalin for 24 h, dehydrated using solutions containing an increasing percentage of ethanol (70–100 %

volume fraction), cleared in Histo-Clear (AS-ONE, Tokyo, Japan), embedded in paraffin under vacuum, divided into 5-mm-thick sections, deparaffinized, and stained with hematoxylin-eosin. The thicknesses of the epidermis and melanin-positive area were measured using a Digimatic Caliper (Mitutoyo Co, Kanagawa, Japan) and Curvimeter (X-PLAN 360 dII, Ushitaka, Tokyo, Japan), respectively.

Statistical analysis

Statistical analyses were performed using ANOVA followed by post hoc Tukey test for multiple comparisons using SPSS (Version 21, SPSS Inc., Chicago, IL). Differences were considered significant at $p < 0.05$.

Results

HPLC standardization of DER

Figure 1A shows the chromatogram for standard rosmarinic acid. The standard calibration curve showed a linear relationship ($R^2 = 0.993$) between the peak area and concentration of rosmarinic acid (Fig. 1C). The inter- and intraday variations were 1.10 and 2.15, respectively. Thus, the HPLC method was accurate and reproducible. The chromatogram (Fig. 1B) for DER showed that rosmarinic acid was the major component. DER was standardized to contain rosmarinic acid of not less than 4.58 ± 0.023 mg%.

HPLC–DAD–MS/MS profiling of DER

The HPLC method separated the DER into 20 different components (Fig. 2), including rosmarinic acid, flavonoids aglycones and glycosides, in addition to diterpenes in 45 min (Table 1).

Rosmarinic acid (peak 6) was identified by comparison with a standard rosmarinic acid, and was the dominant phenolic component. Among the diterpenoids, carnosic acid (peak 19) was the most abundant diterpene and was identified by comparison with the pure standard. Its most diagnostic ions were $[M - H]^-$ and $[M - H{-}CO_2]^-$ at *m/z* 331 and 287, respectively. The diterpene carnosol was also detected (peak 17), and the mass spectra of carnosol gave diagnostic ions in both positive and negative ionization modes. Positive ionization produced $[M + H]^+$ and $[M + Na]^+$ at *m/z* 331 and 352, respectively, in addition to fragments related to the loss of the carboxyl group. Negative ionization produced $[M - H]^-$ and the $[M - H{-}CO_2]^-$ at *m/z* 329 and 285, respectively.

Two diterpenes, rosmanol (peak 11) and epi-rosmanol (peak 12), were also detected with similar retention times as previously reported (Almela et al. 2006; Mulinacci et al. 2011). These two compounds were identified mainly from their UV–Vis and mass spectra. The mass spectrum of rosmanol/epi-rosmanol in negative ionization mode produced $[M - H]^-$ at *m/z* 345, $[M - H{-}CO_2]^-$ at *m/z* 301, and $[M{-}H{-}CO_2{-}H_2O]^-$ at *m/z* 283. The loss of a H_2O molecule was observed only for these compounds with a free OH group on carbon C7. Methyl carnosate (peak 20) was identified by its

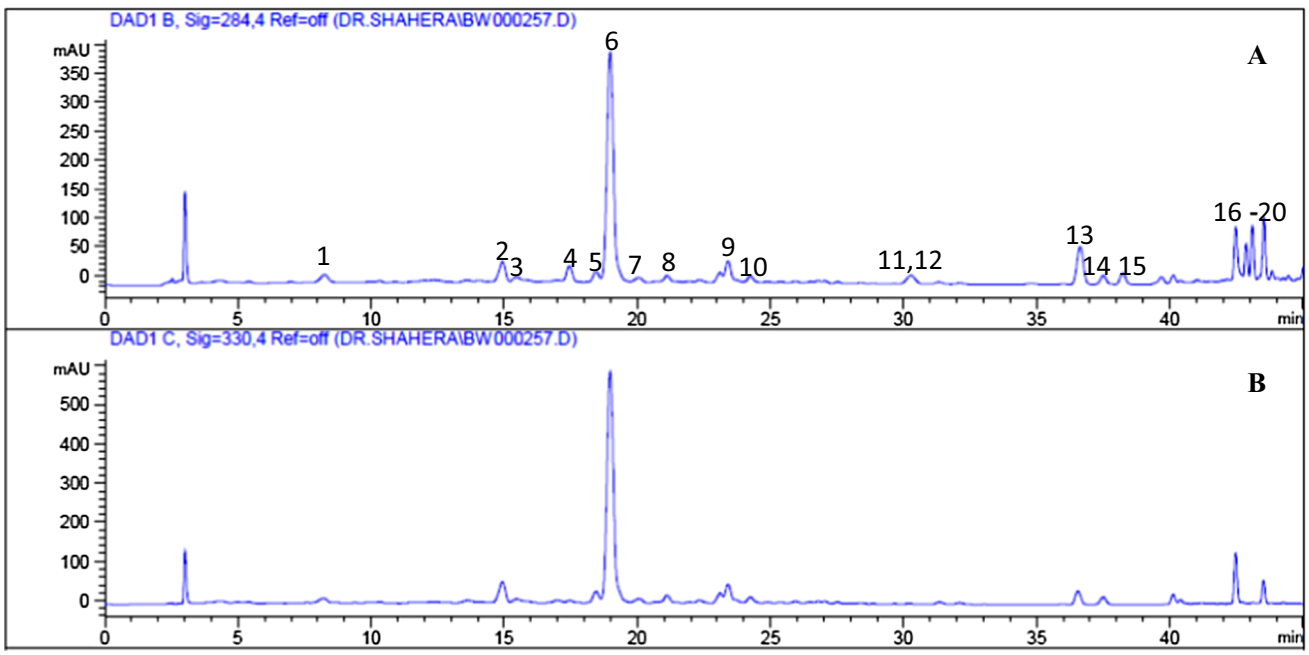

Fig. 2 HPLC chromatograms of DER: **A** at 284 nm and **B** at 330 nm

Table 1 List of compounds identified by their retention time, mass spectra and by the use of standards

Peak no.	Compounds	Rt (min.)	MS (−)	MS (+)
1	Caffeic acid	8.267	179, 135	
2	Apigenin rha-glu	14.941	577	
3	Hesperidin rha-glu	15.08	609, 301	
4	Diosmin rha-glu	17.450	607, 299	
5	Luteolin 7-*O* gluc	18.459	461, 285	
6	Rosmarinic acid	18.992	359, 197, 161	
7	Ispidulin 7-*O* gluc	20.054	461	
8	Cirsimaritin *O*-glu	21.123	475, 315	
9	Flavonoid diglycoside	23.418	653	
10	Isoscutellarein 7-*O*-glu	24.527	461	
11	Rosmanol	30.278	345, 301, 283	
12	Epirosmanol	30.272	345, 301, 283	
13	Cirsimaritin	36.631	313	
14	Flavonoid	37.496		315
15	Genkwanine	40.129	283	285
16	Flavonoid	42.477		351
17	Carnosol	42.872	329, 285	331, 352
18	Metoxytectochrysin	43.102	298	299
19	Carnosic acid	43.535	331, 287	
20	Methyl carnosate	43.840	345, 331, 287	

Rt retention time, *MS* mass spectra, *glu* glucose, *gluc* glucuronic acid, *rha* rhamnose

mass spectrum using $[M - H]^-$ and $[M - H{-}CH_3]^-$ at *m/z* 345 and 331, respectively. By comparison to the mass spectrum of carnosic acid, an ion at *m/z* 287 was attributed to the loss of the CH_3–COO group. Several flavonoid aglycones and glycosides were detected in the DER, and this was in agreement with the literature (Del Bano et al. 2003; Almela et al. 2006). The identified flavonoids were flavones and flavonols, which were identified by their characteristic UV–Vis spectra with two main bands at 260–270 nm and 335–345 nm.

In vitro antioxidant assays of the standardized DER

The in vitro free radical scavenging activity of DER was evaluated against different free radicals. DER showed high free radical scavenging activity against DPPH, $ABTS^{+\cdot}$ and superoxide radicals (Fig. 3) with IC_{50} values of 50.67, 666.67, and 450 μg/mL, respectively. The IC_{50} values for gallic acid were 4.97, 40.25, and 322.12 μg/mL respectively. DER also inhibited bleaching of β-carotene with an IC_{50} of 23.68 μg/mL, and also showed a high ferric chelating ability. By comparison, gallic acid had an IC_{50} 457.12 μg/mL.

Characterization of vesicles

Encapsulation efficiency (EE %)

The highest EE % was obtained with TF4 (98.7 ± 2.8 %) and LP (98.7 ± 3.1 %). The EE % of TF4, which was prepared using Span 60, was higher than that of TF1 (95.9 ± 2.4 %), which was prepared using SDC. It was also much higher than that of TF7 (50.7 ± 5.9 %), which was prepared using Cremophor EL with the same PC:surfactant ratio (95:5 w/w). Statistical analysis showed a significant decrease in the EE % of DER as the surfactant ratio in the TF was increased, and this was irrespective of the surfactant type.

Vesicular size and charge

All TFs and LP formulations showed ranges for the vesicle sizes (133.09–345.7 nm) and low polydispersity indices (0.114–0.366), indicating a homogenous size distribution in the formulation (Table 2). LP vesicles were much smaller size than those of TF. There was a significant decrease in the particle size when using a surfactant with higher hydrophilic lipophilic balance (HLB). This was shown by the decreases in vesicle size from 345.7 ± 17.5 nm (TF4), to 218.8 ± 17.1 nm (TF1), and to 182.08 ± 9.5 nm (TF7) as the HLB of the surfactant was increased from 4.7 (Span 60, TF4), to 16 (SDC, TF1), and to 13 (Cremophor EL, TF7), respectively. Increasing the surfactant ratio resulted in a significant decrease in the vesicle size. Thus, the vesicles prepared with Span 60 with a PC: surfactant ratio of 85:15 were significantly smaller (TF5, 140.6 ± 12.3 nm) than those prepared with a PC: surfactant ratio of 95:5 (TF4, 345.7 ± 17.5 nm). The zeta potentials of the TFs and LP ranged from –12.5 ± 1.5

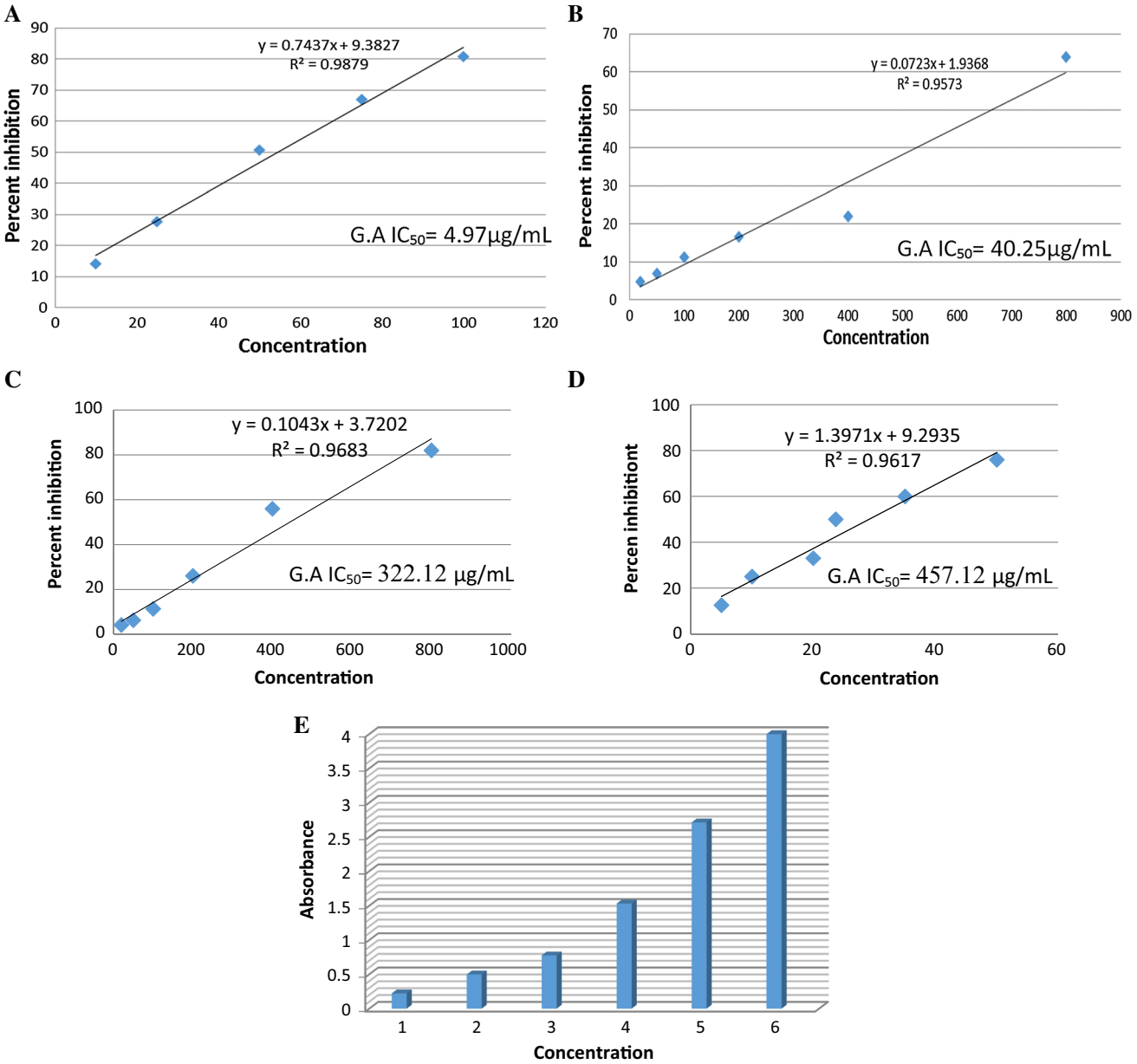

Fig. 3 In vitro antioxidant activity of DER on different free radical scavenging: **A** DPPH, **B** ABTS, **C** Superoxide anion, **D** *Linoleic acid/β-carotene* and **E** Ferric reducing antioxidant power. Concentration of DER in each assay (µg/ml)

to –56.6 ± 6.8 mV (Table 2). TFs (TF1, TF2 and TF3) prepared using SDC as a surfactant had more negative zeta potentials than those prepared with other surfactants. Increasing the amount of surfactant led to a significant increase in the zeta potential. By contrast, the zeta potentials of TFs prepared using Cremophor EL were not affected by the surfactant concentration.

Deformability index

The deformability of all TFs were superior to that of LP (0.5 ± 0.06 mL/s) (Table 2). The deformability indices of the vesicles prepared using SDC increased with increasing surfactant concentration. Among the TFs, TF4 had the highest DI (119 ± 3.4 mL/s), whereas TF7, TF8, and TF9 had the lowest.

These results showed that the TF4 vesicles were the most deformable vesicles, in addition to their acceptable size and EE %. Therefore, TF4 vesicles were selected for further investigation.

Morphology

Photomicrographs of TF4 (Fig. 4A) and LP (Fig. 4B), and TEM micrographs of TF4 (Fig. 4C) and LP (Fig. 4D) were

Table 2 Composition and characterization parameters of different TFs and LP formulations

Formulation	Type of surfactant	Ratio of PC: surfactant/ Chol	EE (%)[a]	z-average (nm)[a]	PDI[a]	Charge (mV)[a]	Deformability index (mL/s)[a]
TF1	SDC	95:5	95.9 ± 2.4	218.8 ± 17.1	0.339	−25.0 ± 5.7	21.4 ± 0.07
TF2	SDC	85:15	67.2 ± 3.8	188.3 ± 16.3	0.303	−50.0 ± 7.4	23.2 ± 0.5
TF3	SDC	75:25	58.4 ± 5.5	160.7 ± 21.3	0.329	−56.6 ± 6.8	35.5 ± 1.1
TF4	Span 60	95:5	98.7 ± 2.8	345.7 ± 17.5	0.360	−21.0 ± 5.6	109.6 ± 3.4
TF5	Span 60	85:15	94.9 ± 5.2	140.6 ± 12.3	0.203	−31.3 ± 6.3	9.6 ± 3.5
TF6	Span 60	75:25	78.1 ± 4.7	115.5 ± 13.4	0.279	−34.8 ± 6.8	16.9 ± 2.2
TF7	Cremophor EL	95:5	50.7 ± 5.9	182.08 ± 9.5	0.257	−29.7 ± 3.3	5.4 ± 0.09
TF8	Cremophor EL	85:15	38.2 ± 6.4	147.94 ± 8.6	0.260	−28.0 ± 1.6	2.3 ± 0.03
TF9	Cremophor EL	75:25	35.9 ± 5.7	133.09 ± 4.5	0.366	−27.3 ± 2.4	1.2 ± 0.9
LP	–	85:15	98.7 ± 3.1	107.8 ± 11.3	0.114	−12.5 ± 1.5	0.5 ± 0.06

Ratio of PC: surfactant and ratio of PC: Chol is (w/w)

TF transferosomes, *LP* liposomes, *SDC* sodium deoxycholate, *PC* phosphatidylcholine, *Chol* cholesterol

[a] Values are expressed as mean ± SD ($n = 3$)

recorded. These micrographs showed that TF4 and LP were spherical. AFM of TF4 showed many spherical vesicles (Fig. 4E), with cross sections of 100 and 200 nm (Fig. 4F).

In vitro skin permeation and retention studies

The results of in vitro skin permeation studies (Table 3; Fig. 5) showed that TF4 had a rate of permeation (R) of 0.53 ± 0.3 μg/h, lag time of 18.2 ± 2.5 min, and Q_{24} of 53.04 ± 3.9 μg. The amount of DER retained in the skin after the permeation study was 10.82 ± 2.0 μg/cm^2. For LP, R was 0.24 ± 0.1 μg/h, the lag time was 27.3 ± 1.3 min and Q_{24} was 22.24 ± 5.1 μg. The amount of DER retained in the skin after the permeation study was 4.53 ± 1.6 μg/cm^2. The above results were compared with the permeation profile for unencapsulated DER through rat skin, which had significantly lower R (0.02 ± 1.2 ug/h) and Q_{24} (7.97 ± 0.5 μg) and a significantly longer lag time (35.1 ± 0.9 min). This proved that encapsulation of DER inside LPs or TFs enhanced its permeation through rat skin, with TFs showing enhanced permeation compared with LPs.

In vivo anti-wrinkle activity

Measurement of skin wrinkles on UVB-irradiated mice

Compared with group I mice (control group no irradiation), expression of MMP-2 and MMP-9 increased with chronic UVB irradiation (Table 4). The increase in expression of MMP-2 was significantly inhibited by DER (50 or 100 mg, twice daily) and TF4 compared with the group that underwent UVB irradiation but were not treated with any form of DER. However, topical application of 20 mg of DER twice daily for 2 weeks did not significantly affect the expression of MMP-2 and MMP-9. According to Bissett et al. (1987) scoring, TF4 (20 mg of DER) inhibited MMP-2 expression (0.23 ± 0.01) better than DER alone at the same dose (20 mg), and inhibited MMP-9 expression (0.52 ± 0.09) at a similar level to DER at 100 mg. This indicated that the anti-wrinkle activity of DER was enhanced when encapsulated within TFs. By contrast, TF4 without encapsulated DER did not show significant inhibition of either MMP-2 or MMP-9 expression. This excluded the possibility that the TF4 vesicle itself showed anti-wrinkle activity.

Histopathological examination of UVB-irradiated mice

Images of the skin from untreated and treated mice were recorded (Fig. 6A–I). The mice in the control group (group I) had normal skin (Fig. 6A, H). Skin specimens showed two layers of the epidermis, and no melanin was observed (Fig. 6I). Collagen was mature in both superficial and deep areas of the dermis, and the elastic fibers were of normal thickness with no fragmentation. Compared with group I, skin from the UVB-irradiated mice (group II) showed significant thickening of the epidermis (Fig. 6B, H) and an increase in melanin production in the basal layer (Fig. 6I). Topical application of DER (20 mg) showed a non-significant decrease in the epidermal thickness (Fig. 6C, H), and also reduced the area of melanin granule expression (Fig. 6I). Twice daily topical application of DER (50 mg, Fig. 6D), DER (100 mg, Fig. 6E) and TF4 containing 20 mg of DER (Fig. 6F) significantly decreased the thickness of epidermis (Fig. 6H). In addition, DER (50 mg, 100 mg and TF4 containing 20 mg) significantly reduced the area of melanin granule expression (Fig. 6I). The non-

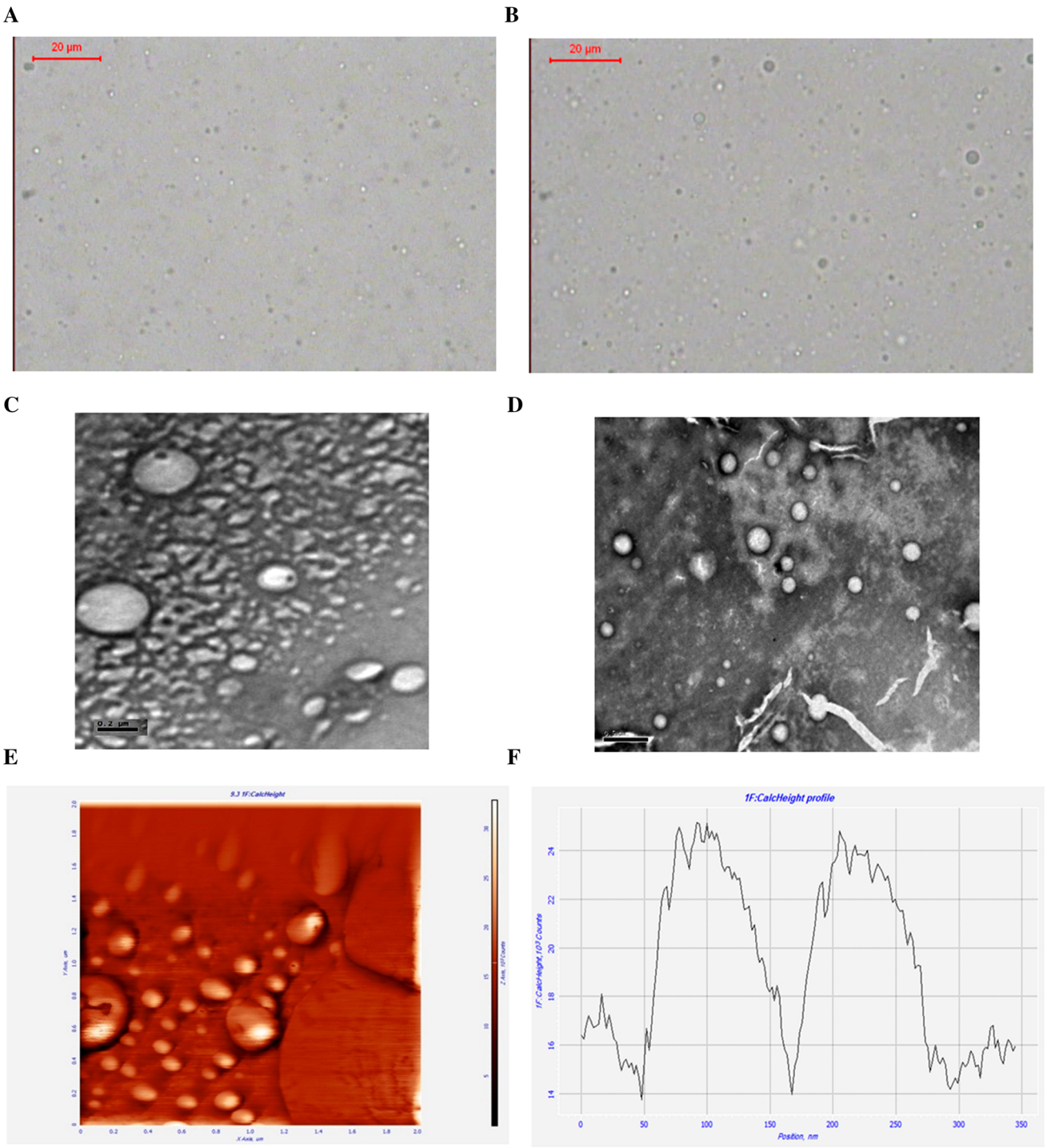

Fig. 4 Photographs of TF4 and LP: **A** Photomicrograph of TF4 (*bar* 20 µm), **B** Photomicrograph of LP (*bar* 20 µm); **C** TEM micrograph of TF4 (*bar* 0.2 µm), **D** TEM micrograph of LP (*bar* 0.2 µm); **E** AFM image of TF4, **F** Graph showing the size of vesicles

medicated formula (i.e. TF4 without DER) did not show any effect on the UVB-irradiated skin (Fig. 6G). Notably, the effects of TF4 containing 20 mg of DER on epidermis thickness and melanin granule expression were better than those of DER alone at the same dose.

Discussion

Standardized herbal extracts are required so that uniform products can be prepared for clinical trials. Herein, DER was standardized by HPLC using rosmarinic acid as a

Table 3 Permeation parameters of TF, LP and DER alone through rats' skin

Formulation	Amount of DER permeated after 24 h (Q_{24}) (μg)[a]	Rate of skin permeation (R) (μg/h)[a]	L_t (min)[a]	Amount of DER retained in the skin (μg/cm^2)[a]
TF4	53.04 ± 3.9	0.53 ± 0.3	18.2 ± 2.5	10.82 ± 2.0
LP	22.24 ± 5.1	0.24 ± 0.1	27.3 ± 1.3	4.53 ± 1.6
DER alone	7.97 ± 0.5	0.02 ± 1.2	35.1 ± 0.9	–[b]

[a] Values are expressed as mean ± SD ($n = 3$)

[b] Amount of DER retained in rats' skin after permeation of DER alone was not determined

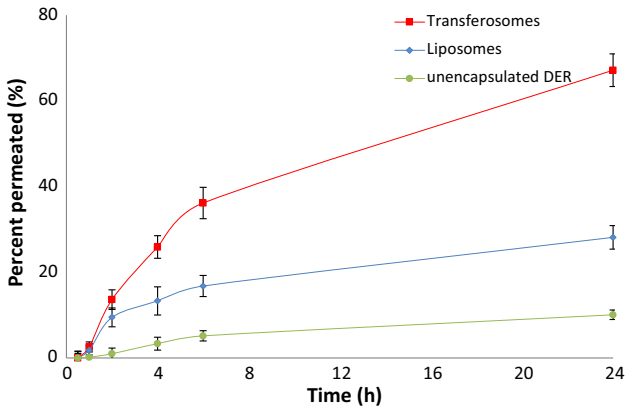

Fig. 5 Skin permeation profile of (■) TF4, (◆) LP and (●) DER alone through excised rats' skin. Values are expressed as mean of three experiments; h, hours

chemical marker. HPLC–DAD-MS/MS analysis of the extract was performed to identify its active constituents. This could be used to provide a more consistent, and effective product with chemical analysis to confirm the presence and ratios of characteristic constituents.

Skin aging can be caused by intrinsic or extrinsic processes. Intrinsic skin aging occurs because of continual formation of ROS. Extrinsic aging develops because of environmental factors, such as exposure to UV radiation (Kim et al. 2011). To evaluate the anti-wrinkle potential of DER, it was tested against both intrinsic and extrinsic factors.

DER had a significant antioxidant effect, which can be attributed to its major phenolic component (i.e. rosmarinic acid), which reportedly has free radical scavenging activity (Luis and Johnson 2005). The presence of the diterpenes carnosic acid and carnosol, which are two natural compounds with antioxidant activity (Aruoma et al. 1992), may add to the activity of DER. The diterpene rosmanol, which reportedly has powerful antioxidant activity (Nakatani and Inatani 1981), may also contribute to the antioxidant activity of DER.

Free radicals can attack molecules and result in cell damage, and that can cause skin aging. Antioxidants have the ability to neutralize free radicals and prevent this damage. This is why natural antioxidants are included in anti-aging skin care products. Our findings support the use of DER in skin care products as a natural antioxidant.

LPs possessed high EE % because of the presence of Chol. Compared with TFs which lacks Chol, this Chol increases the packing ability of the liposomal vesicles, reduces the bilayer permeability, and increases the amount of DER they can enclose. TFs were prepared using Span 60 (HLB 4.7), Cremophor EL (HLB 13) or SDC (HLB 16). Because of the lipophilic nature of the DER, TFs prepared using low HLB surfactants, such as Span 60, were better for encapsulation. As the HLB of a surfactant increases, its affinity to the lipophilic drug decreases (Lei et al. 2013). TFs containing Cremophor EL had the lowest EE % because this surfactant is liquid, whereas the other two surfactants are solid. An increase in surfactant

Table 4 Results of wrinkle scores, MMP-2 and MMP-9 for different mice groups

Group no.	Treatment	Wrinkle score[a]	MMP-2	MMP-9
I	Control	0.00 ± 0.00	0.12 ± 0.02	0.54 ± 0.03
II	UVB irradiated	3.70 ± 0.23	0.72 ± 0.08	1.28 ± 0.20
III	DER (20 mg/twice daily/15 weeks)	2.45 ± 0.23	0.62 ± 0.08	0.79 ± 0.20
IV	DER (50 mg/twice daily/15 weeks)	2.08 ± 0.22[b]	0.37 ± 0.05[b]	0.67 ± 0.09[b]
V	DER (100 mg/twice daily/15 weeks)	1.85 ± 0.36[b]	0.32 ± 0.06[b]	0.49 ± 0.09[b]
VI	TF4 (20 mg DER/twice daily/15 weeks	1.93 ± 0.17[b]	0.23 ± 0.01[b]	0.52 ± 0.09[b]
VII	Non-medicated TF4 twice daily/15 weeks	2.55 ± 0.26	0.54 ± 0.10	0.88 ± 0.06

Values are expressed as mean ± SE ($n = 5$)

[a] Wrinkle scoring was carried out adopting Bissett's grading scale [27]

[b] Significantly different from UVB-irradiated mice (control) at $p < 0.05$

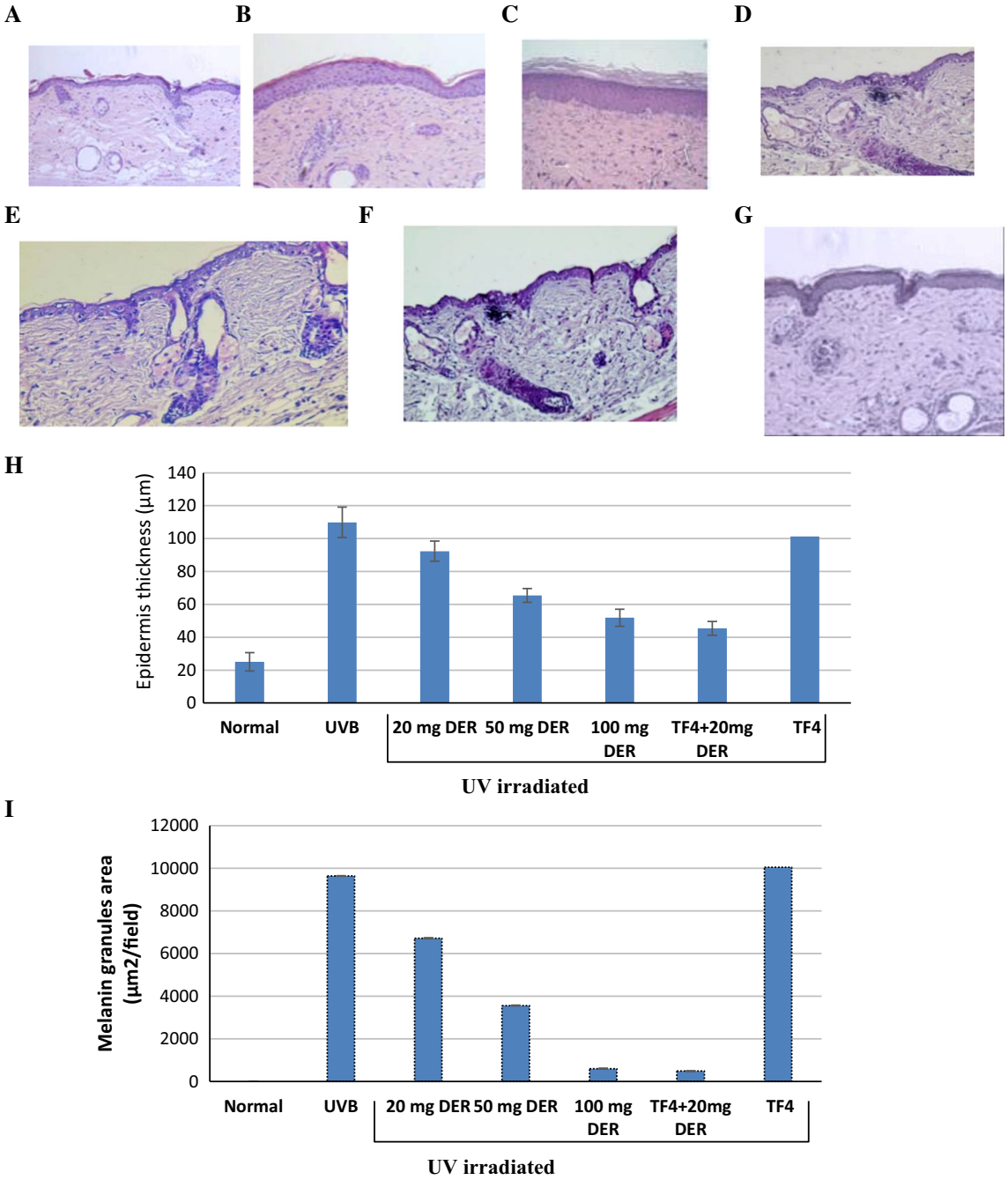

Fig. 6 Histopathological examination of mice skin stained with hematoxylin-eosin (HE). **A** Normal skin; **B** UVB-irradiated skin; **C** UVB-irradiated skin and treated with 20 mg DER; **D** UVB-irradiated skin and treated with 50 mg DER; **E** UVB-irradiated skin and treated with 100 mg DER; **F** UVB-irradiated skin and treated with TF4 containing 20 mg DER; **G** UVB-irradiated skin and treated with non-medicated TF4; **H** Effect of different treatments on the epidermis thickness; **I** Effect of different treatments on melanin granules area

concentration will destabilize the lipid bilayer (Fang et al. 2008; Duangjit et al. 2011), with possible pore formation leading to poor EE % (Gupta et al. 2005). Moreover, the presence of surfactants solubilizes DER in the vesicle for diffusion into the aqueous medium.

Surfactants interact with lipid groups to increase the packing density and surface free energy, which allows fusion between lipid bilayers, and produce large vesicles (Yoshioka et al. 1994; Lichtenberg et al. 2000). In the present study, because Span 60 was the most hydrophobic surfactant used, the TFs produced with Span 60 were the largest.

PC is zwitterionic with an isoelectric point (pI) between 6 and 7 (Chain and Kemp 1934). In the present study, on lipid hydration with PBS (pH 7.4) during formation of LP

and TFs, the pH increased above the pI leaving PC with a net negative charge. All the surfactants used in this study were nonionic. The exception was SDC, which was anionic and increased the negative charge of the vesicle. Vesicles with higher negative charges usually have better stability and improved skin permeation compared to those with lower negative charges (Cevc et al. 1998).

The TFs were more deformable than LP because the surfactants used in the TFs contributed to their deformability. By contrast, LP was produced using Chol, which tends to form rigid vesicles. The DI increased with increasing surfactant concentration because of fluidization of the lipid bilayer (Mahor et al. 2007; Irfan et al. 2012). Compared with the other vesicles, TF7, TF8 and TF9 had lower DIs because Cremophor is large (MW 3,000 Da), which made these vesicles less flexible and less deformable.

The enhanced permeation rate and amount of DER that permeated into the skin from TF4 compared with LP and DER alone could be attributable to the elasticity of the vesicular membrane of the TFs, which made them adaptable to stress. Furthermore, the TF4 vesicles were able to compress to pass through the small pores of the skin easily and reach the receptor medium intact. Consequently, TF4 vesicles containing DER had a lower lag time than DER alone. Compared with LP, TF4 significantly enhanced permeation of DER through rat skin, and this increased the levels of the extract retained in the skin for later release.

We hypothesized that the anti-wrinkle activity of DER observed in our model study could be caused by bioactive metabolites. First, HPLC–MS/MS analysis showed that the major component of DER was rosmarinic acid, in addition to other phenolics and flavonoids. Carnosic acid and carnosol, which are potent antioxidants, were also detected (Frankel et al. 1996). In addition, the diterpene rosmanol, which is a powerful free radical scavenger, was present in the extract (Nakatani and Inatani 1981). These antioxidant metabolites are expected to scavenge and directly remove ROS, which will attenuate the main cause of photo-aging induced by chronic UV irradiation.

In summary, elastic TFs encapsulating DER were formulated and passed through the skin barrier to provide good skin permeability and retention time of DER in the skin. The TFs allowed the herbal extract to exert a sustained anti-wrinkle effect. The anti-wrinkle activity of DER may be attributable to the antioxidant activity of its different constituents, which were identified by HPLC–DAD-MS/MS. These findings will be valuable for the development of commercial skin care formulations. However, further clinical studies and comparison to other anti-wrinkle treatment delivery methods are required.

Acknowledgments The authors would like to thank Associate Professor Dr. Anka Klingner, Physics Department, Faculty of Basic Science, German University in Cairo, Al-Tagmoa Al-Khames, New Cairo, Egypt for assistance with the AFM measurements. The authors would also like to thank Prof. Dr. Wafaa Amer,Botany Department, Faculty of Science, Cairo University, Egypt for authentication of the plant material. The authors are also grateful to Prof. Dr. Hesham El-Askary, Pharmacognosy Department, Faculty of Pharmacy, Cairo University for performing the HPLC analysis.

Compliance with ethical standards

Conflict of interest All authors declare no conflict of interest.

References

Almela L, Sánchez-Muñoz B, Feránndez-López AJ, Roca MJ, Rabe V (2006) Liquid chromatograpic–mass spectrometric analysis of phenolics and free radical scavenging activity of rosemary extract from different raw material. Chromatogr A 1120:221–229

Alzomor AK, Al-Absi NM, Al-Zubaidi SM (2015) Extraction and formulation of rosemary as anti-wrinkle cream and gel. Eur J Biomed Pharm Sci 2:1–16

Aruoma O, Halliwell B, Aeschbach R, Löliger J (1992) Antioxidant and pro-oxidant properties of active rosemary constituents: carnosol and carnosic acid. Xenobiotica 22:257–268

Bangham AD, Horn TN (1964) Negative staining of phospholipids and their structural modification by surface-active agents as observed in the electron microscope. J Mol Biol 8:660–668

Birkedal-Hansen H (1995) Proteolytic remodeling of extracellular matrix. CurrOpin Cell Biol 7:728–735

Bissett DL, Hannon DP, Orr TV (1987) An animal model of solar-aged skin: histological, physical, and visible changes in UV-irradiated hairless mouse skin. Photochem Photobiol 46:367–378

Calabrese V, Scapagnini G, Catalano C, Dinotta F, Geraci D, Morganti P (2000) Biochemical studies of a natural antioxidant isolated from rosemary and its application in cosmetic dermatology. Int J Tissue React 22:5–13

Cao H, Cheng WX, Li C, Pan XL, Xie XG, Li TH (2005) DFT study on the antioxidant activity of rosmarinic acid. J Mol Struct 19:177–183

Cevc G, Gebauer D, Stieber J, Schatzlein A, Blume G (1998) Ultraflexible vesicles, transfersomes, have an extremely low pore penetration resistance and transport therapeutic amounts of insulin across the intact mammalian skin. BiochimBiophysActa 1368:201–215

Chain E, Kemp I (1934) The isoelectric points of lecithin and sphingomyelin. Biochem J 28:2052–2055

Del Bano MJ, Lorente J, Castillo J, Benavente-Garcia O, Del Rio JA, Otuno A, Quirin KW, Dieter G (2003) Phenolic diterpenes, flavones, and rosmarinic acid distribution during the development of leaves, flowers, stems, and roots of *Rosmarinusofficinalis*. J Agric Food Chem 51:4247–4253

Delazar A, Byres M, Gibbons S, Kumarasamy Y, Modarresi M, Nahar L, Shoeb M, Sarker SD (2004) Iridoid glycosides from *Eremostachysglabra*. J Nat Prod 67:1584–1587

Duangjit S, Opanasopit P, Rojanarata T, Ngawhirunpat T (2011) Characterization and in vitro skin permeation of meloxicam-loaded liposomes versus transferosomes. J Drug Del. doi:10.1155/2011/418316

Elizabeth K, Rao MNA (1990) Oxygen radical scavenging activity of curcumin. Int J Pharm 58:237–240

Fang YP, Tsai YH, Wu PC, Huang TB (2008) Comparison of 5-aminolevulinic acid-encapsulated liposome versus ethosome for skin delivery for photodynamic therapy. Int J Pharm 356:144–152

Fisher GJ, Datta SC, Talwar HS, Wang ZO, Varani J, Kang S, Voorhees JJ (1996) Molecular basis of sun-induced premature skin ageing and retinoid antagonism. Nature 379:335–339

Frankel EN, Huang SW, Aeschbach R, Prior E (1996) Antioxidant activity of a rosemary extract and its constituents, carnosic acid, carnosol, and rosmarinic acid, in bulk oil and oil-in-water emulsion. J Agric Food Chem 44:131–135

Gupta PN, Mishra V, Rawat A, Dubey P, Mahor S, Jain S, Chatterji DP, Vyas SP (2005) Non-invasive vaccine delivery in transfersomes, niosomes and liposomes: a comparative study. Int J Pharm 293:73–82

Inatani R, Nakatani N, Fuwa H (1983) Antioxidative effect of the constituents of Rosemary (*Rosmarinusofficinalis* L.) and their Derivatives. Agric Biol Chem 47:521–528

Irfan M, Verma S, Vam A (2012) Preparation and characterization of ibuprofen loaded transferosome as a novel carrier for drug delivery system. Asian J Pharm Clin Res 5:162–165

Jia-You F, Yann-Lii L, Chia-Chun C, Chia-Hsuan L, Yi-Hung T (2004) Lipid nano/submicron emulsion as vehicle for topical flurbiprofen delivery. Drug Del 11:97–105

Kim DS, Jeon BK, Mun YJ, Kim YM, Lee YYE, Woo WH (2011) Effect of *Dioscoreaaimadoimo* on anti-aging and skin moisture capacity. J Orient Physiol Pathol 25:425–430

Koleva RI, van Beek TA, Linssen JP, de Groot A, Evstatieva LN (2002) Screening of plant extracts for antioxidant activity: a comparative study on three testing methods. Phytochem Anal 13:8–17

Kumaran A, Karunakaran RJ (2006) Antioxidant activities of the methanol extract of *Cardiospermumhalicacabum*. Pharm Biol 44:146–151

Lei W, Yu C, Lin H, Zhou X (2013) Development of tacrolimus-loaded transfersomes for deeper skin penetration enhancement and therapeutic effect improvement in vivo. Asian J PharmSci 8:336–345

Lichtenberg D, Opatowski E, Kozlov MM (2000) Phase boundaries in mixtures of membrane-forming amphiphiles and micelle-forming amphiphiles. BiochimBiophysActa 1508:1–19

Luis JC, Johnson CB (2005) Seasonal variations of rosmarinic and carnosic acids in rosemary extracts. Analysis of their in vitro antiradical activity. Span J Agric Res 3:106–112

Mahor S, Rawat A, Dubey PK, Gupta PN, Khatri K, Goyal AK, Vyas SP (2007) Cationic transfersomes based topical genetic vaccine against hepatitis B. Int J Pharm 340:13–19

Manconi M, Caddeo C, Sinico C, Valenti D, Mostallino C, Biggio G, Fadda AN (2011) *Ex-vivo* skin delivery of diclofenac by transcutol containing liposomes and suggested mechanism of vesicle–skin interaction. Eur J Pharm Biopharm 78:27–35

Modi CD, Bharadia PD (2012) Transfersomes new dominants for transdermal drug delivery. Am J Pharm Tech Res 2:71–91

Mulinacci N, Innocenti M, Bellumori M, Giaccherini C, Martini V, Michelozzi M (2011) Storage method, drying processes and extraction procedures strongly affect the phenolic fraction of rosemary leaves: an HPLC/DAD/MS study. Talanta 85:67–176

Muñoz-Muñoz JL, Garcia-Molina F, Ros E, Tudela J, García-Canovas F, Rodriguez-Lope JN (2013) Prooxidant and Antioxidant Activities of Rosmarinic Acid. J Food Biochem 37:396–408

Mura P, Maestrelli F, Gonzalez-Rodriguez ML, Michelacci J, Ghelardini C, Rabasco AM (2007) Development, characterization and in-vivo evaluation of benzocaine-loaded liposomes. Eur J Pharm Biopharm 67:86–95

Nakatani N, Inatani R (1981) Structure of rosmanol, a new antioxidant from rosemary (*Rosmarinus officinalis* L.). Agric Bio Chem 45:2385–2386

Ozgen M, Reese RN, Tulio AZ, Scheerens JC, Miller AR (2006) Modified 2,2-Azino-bis-3-ethylbenzothiazoline-6-sulfonic Acid (ABTS) method to measure antioxidant capacity of selected small fruits and comparison to ferric reducing antioxidant power (FRAP) and 2,2′-diphenyl-1-picrylhydrazyl (DPPH) methods. J Agric Food Chem 54:1151–1157

Pinnell SR (2003) Cutaneousphotodamage, oxidative stress, and topical antioxidant protection. J Am Acad Dermatol 48:1–19

Sumiyoshi M, Kimura Y (2009) Effects of turmeric extract (*Curcuma longa*) on chronic ultraviolet B irradiation—induced skin damage in melanin-possessing hairless mice. Phytomedicine 16:1137–1143

Takao T, Watanabe N, Yagi I, Sakata K (1994) A simple screening method for antioxidants and isolation of several antioxidants produced by marine bacteriafrom fish and shellfish. Biosci Biotech Biochem 58:1780–1783

Troncoso N, Sierra H, Carvajal L, Delpiano P, Günther G (2005) Fast high performance liquid chromatography and ultraviolet–visible quantification of principal phenolic antioxidants in fresh rosemary. J Chromatogr A 1100:20–25

Tsai JC, Huang GJ, Chiu TH, Huang SS, Huang SC, Huang TH, Lai SC, Lee CY (2011) Antioxidant activities of phenolic components from various plants of *Desmodium*specie. Afr J Pharm Pharmacol 5:468–476

Verma DD, Verma S, Blume G, Fahr A (2003) Particle size of liposomes influences dermal delivery of substances into skin. Int J Pharm 258:141–151

Yoshioka T, Sternberg BF, Lorence AT (1994) Preparation and properties of vesicles (niosomes) of sorbitan monoesters (Span 20, 40, 60 and 80) and a sorbitantriester (Span 85). Int J Pharm 105:105–106

Zhang PJ, Wei WH, Zhou Y, Li YQ, Wu XA (2012) Ethosomes, binary ethosomes and transfersomes of terbinafine hydrochloride: a comparative study. Arch Pharm Res 35:109–117